

This item was submitted to Loughborough's Institutional Repository (<https://dspace.lboro.ac.uk/>) by the author and is made available under the following Creative Commons Licence conditions.



CC creative commons
COMMONS DEED

Attribution-NonCommercial-NoDerivs 2.5

You are free:

- to copy, distribute, display, and perform the work

Under the following conditions:

 **Attribution.** You must attribute the work in the manner specified by the author or licensor.

 **Noncommercial.** You may not use this work for commercial purposes.

 **No Derivative Works.** You may not alter, transform, or build upon this work.

- For any reuse or distribution, you must make clear to others the license terms of this work.
- Any of these conditions can be waived if you get permission from the copyright holder.

Your fair use and other rights are in no way affected by the above.

This is a human-readable summary of the [Legal Code \(the full license\)](#).

[Disclaimer](#) 

For the full text of this licence, please go to:
<http://creativecommons.org/licenses/by-nc-nd/2.5/>

1 **Hardened properties of high-performance printing concrete**

2

3

4 T. T. Le, S. A. Austin, S. Lim, R. A. Buswell, R. Law A. G. F. Gibb, T. Thorpe

5

6 *Department of Civil and Building Engineering, Loughborough University,*

7 *Loughborough, Leicestershire, LE11 3TU, United Kingdom*

8

9

10 **Abstract**

11

12

13 This paper presents the hardened properties of a high-performance fibre-reinforced
14 fine-aggregate concrete extruded through a 9 mm diameter nozzle to build layer-by-
15 layer structural components in a printing process. The printing process is a digitally
16 controlled additive method capable of manufacturing architectural and structural
17 components without formwork, unlike conventional concrete construction methods.

18 The effects of the layering process on density, compressive strength, flexural
19 strength, tensile bond strength and drying shrinkage are presented together with the
20 implication for mix proportions. A control concrete (mould-cast specimens) had a
21 density of approximately 2,250 kg/m³, high strength (107 MPa in compression, 11
22 MPa in flexure) and 3 MPa in direct tension, together with a relatively low drying
23 shrinkage of 175 microns (cured in water) and 855 microns (cured in a chamber at
24 20°C and 60% relative humidity) at 184 days. In contrast well printed concrete had a
25 density of 2,350 kg/m³, compressive strength of 75-102 MPa, flexural strength of 6-
26 17 MPa depending on testing direction, and tensile bond strength between layers
27 varying from 2.3-0.7 MPa, reducing as the printing time gap between layers

28 increased. The well printed concrete had significantly fewer voids greater than
29 0.2mm diameter (1.0%) when compared with the mould-cast control (3.8%), whilst
30 samples of poorly printed material had more voids (4.8%) mainly formed in the
31 interstices between filaments. The additive extrusion process was thus shown to
32 retain the intrinsic high performance of the material.

33

34

35 *Key words:* Additive Manufacturing; Bond Strength (C); Compressive Strength (C);
36 High-Performance Concrete (E); Tensile Properties (C)

37

38

39 **1. Introduction**

40

41

42 A high performance printing concrete has been developed for an innovative freeform-
43 construction concrete-printing process [1, 2]. The concrete used some advantages of
44 self-compacting concrete [3, 4] and sprayed concrete [5, 6] for optimisation of the mix
45 proportions to suit the innovative process. The concrete printing process and the
46 fresh properties of the concrete, including the optimisation of mix proportions,
47 extrudability, workability, open time and buildability are reported elsewhere [7, 8].

48

49

50 The concrete printing process uses an additive, layer-based, manufacturing
51 technique to build complex geometrical shapes without formwork and thus has a
52 unique advantage over conventional construction methods. Additive manufacturing
53 (AM) has been applied to the production of cement composites such as Contour
54 Crafting [9] and D-Shape (Monolite) [10]. Contour Crafting is based upon extruding a
55 cement-based paste against a trowel that creates a smooth surface finish through the

56 build up of subsequent layers. The D-Shape involves a powder deposition process,
57 where each layer of build material is deposited to the desired thickness, compacted
58 and then nozzles mounted on a gantry frame deposit the binder where the part is to
59 be made solid. Other applications of AM include the medical field XXXX [11-13].

60 Work to overcome the poor water resistance of commercially available materials ,
61 which is problematic for applications including biomedical processing [13].

62

63

64 Briefly, in the concrete printing process, components are designed as volumetric
65 objects using 3D modelling software. They are sliced and represented as a series of
66 two dimensional layers. The data are exported to a printing machine layer-by- to print
67 structural components by the controlled extrusion of a concrete. The rheology must
68 allow its extrusion through a printing head incorporating a 9 mm diameter nozzle to
69 form small concrete filaments. As they are laid, the filaments bond together to form
70 each layer and to the previous layers to build 3D components.

71

72

73 The layered structure is likely to be anisotropic as voids can form between filaments
74 to weaken the structural capability. The bond between filaments, as well as between
75 layers, probably influences the hardened properties of concrete components.

76 Therefore, a high strength in compression and flexure as well as tensile bond are the
77 main targets in developing this concrete. Additionally, a low shrinkage is essential as
78 the freeform components are built without formwork and this could accelerate water
79 evaporation in the concrete and result in cracking.

80

81

82 This paper presents the hardened properties comprising density, compressive and
83 flexural strengths, tensile bond strength and drying shrinkage. Void measurement

84 was also carried out to further understand the hardened properties. It compares the
85 performance of conventionally cast (the control) and in-situ printed states,
86 considering where appropriate the anisotropy resulting from the extrusion process.

87

88

89 **2. Experimental Programme**

90

91

92 **2.1. Specimen manufacture**

93

94

95 In this research, the specimens were manufactured in both mould-cast and printed
96 states. The test results would show clearly the impact of the concrete printing
97 process on the hardened properties of concrete.

98

99

100 *2.2.1. Mould cast control samples*

101

102

103 All control specimens were cast in moulds and complied with the respective BS EN
104 standards used to measure the properties. Compressive strength specimens were
105 cast in 100mm cube steel moulds complied with BS EN 12390-3:2009 [14]. Flexural
106 strength specimens were cast in 100x100x500 mm steel moulds complied with BS
107 EN 12390-5:2009 [15]. Tensile strength specimens were cored from 150mm mould-
108 cast cubes to comply with BS EN 14488-4:2005+A1:2008 [16]. Shrinkage specimens
109 were cast in 75x75x220mm steel moulds in accordance with BS EN 12617-4:2002
110 [17].

111

112

113 **2.2.2. Printed samples**

114

115

116 The printed specimens were manufactured by sawing and coring from printed
117 components including 350x350x120 mm slabs, 500x350x120mm slabs, a trial curvy-
118 shape bench with 2000/1000/63 mm length/width/thickness and 500x100x200 mm
119 beams (see Experimental section).

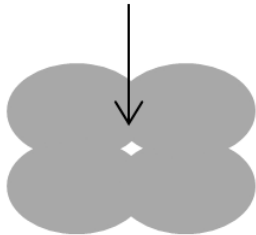
120

121 As expected, the process had the potential to create small voids in the interstices
122 between the filaments (Figure 1(a)). A cross section of a poorly manufactured
123 specimen is shown in Figure 1(b). Careful design and control of the mix rheology and
124 printing process avoids such macro effects, but the sample serves to illustrate the
125 potential for longitudinal flaws and the resulting anisotropy that this paper explores.

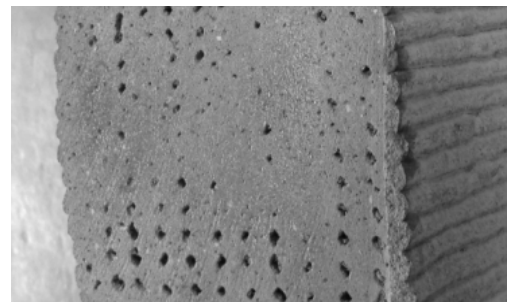
126

127

A void between 4 filaments



a) Four filaments may form a void



b) Poor printing example with obvious voids between filaments

128 Figure 1. Voids formed between filaments resulting from a poorly executed printing
129 process

130

131

132 **2.2. Materials and mix proportions**

133

134

135 The mix design aimed to meet the requirements of both the fresh and hardened
136 states. The former comprises printability, workability, open time and buildability. The
137 hardened performance includes the compressive and flexural strengths of both cast
138 and printed specimens. The mix design targeted a compressive strength of over 100
139 MPa and a flexural strength of over 10 MPa at 28 days for mould-cast specimens. A
140 2 mm maximum size sand was selected because of the small nozzle diameter (9mm)
141 required to give a high printing resolution; cement CEM I 52.5, fly ash conforming to
142 BS EN 450 and undensified silica fume formed the binder component. The gradings
143 of sand, cement, fly ash and silica fume, measured by a Mastersizer 2000 machine,
144 were combined in various proportions to form smooth grading curves of potential
145 mixtures.

146

147

148 Dry components were mixed with water and a polycarboxylate-based
149 superplasticiser to lower the water/binder ratio and hence increase its workability and
150 strength. A retarder, formed by amino-tris (methylenephosphonic acid), citric acid and
151 formaldehyde, maintained sufficient open time, facilitating a constant flow during
152 printing. The concrete also contained 12/0.18 mm length/diameter polypropylene
153 micro fibres to reduce the possibility of plastic shrinkage. The optimum mix was
154 found to be one with the lowest content of binder that could be printed and built with
155 the recommended dosage of fibres from the supplier (i.e. 1.2 kg/m³) that gained the
156 target strengths.

157

158

159 The optimisation process resulted in a mix with a 60:40 sand:binder ratio, comprising
160 70% cement, 20% fly ash and 10% silica fume, plus 1.2 kg/m³ micro polypropylene

161 fibres [7, 8]. The water:binder ratio was 0.26. This mix required 1% superplasticiser
162 and 0.5% retarder to attain an optimum workability of 0.55 kPa shear strength, an
163 optimum open time of up to 100 minutes and the ability to build a large number of
164 layers with various filament groups. The compressive strength of this mix, determined
165 by casting 100 mm cube specimens, was 20, 80, 107 and 125 MPa, at 1, 7, 28 and
166 56 days respectively. A variety of parts were printed with mould-cast controls, and
167 specimens extracted to determine the effects of this AM process on key properties,
168 namely density, compressive strength, flexural strength, tensile bond strength and
169 drying shrinkage. Except where stated, all properties reported are with these mix
170 proportions.

171

172

173 **2.3. Experimental procedures**

174

175

176 *2.3.1. Density*

177

178

179 The density of mould-cast and printed specimens were averaged from at least three
180 specimens, the former complying with BS EN 12390-7:2009 [18]. For printed
181 concrete, 100 mm cube specimens were sawn from 350x350x120 mm and
182 500x350x120 mm printed slabs to measure the density as for the mould-cast
183 specimens. The results were verified with 58 mm diameter cores in the investigation
184 of tensile bond strength.

185

186

187 *2.3.2. Compressive strength*

188

189

190 Compressive strength was measured in both mould-cast and printed specimens.

191 Most specimens were 100 mm cubes. Mould-cast specimens were cured in a 20°C

192 water tank and tested at 1, 7 and 28 day ages to monitor the strength development

193 with time.

194

195

196 For printed elements, 100 mm cube specimens were extracted from one

197 350x350x120 mm slab and three 500x350x120 mm slabs (Figures 2 and 4). The

198 slabs were cured under damp hessian, wrapped in plastic sheeting. Nine cubes were

199 extracted from the 350x350x120 mm slab and loaded in one of three directions:

200 direction I for specimens 1-3; direction II for specimens 4-6; and direction III for

201 specimens 7-9 (Figure 2). Nine cubes extracted from three 500x350x120 mm slabs

202 were tested at the same loading directions of the flexural beam specimens (Figure 4).

203

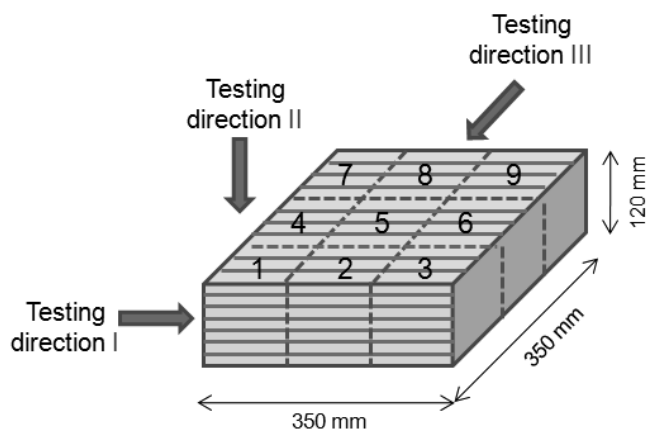
204

205 All 100 mm cube specimens were tested in accordance with BS EN 12390-3:2009

206 [14]. Printed specimens were capped with a high strength gypsum-based plaster.

207

208

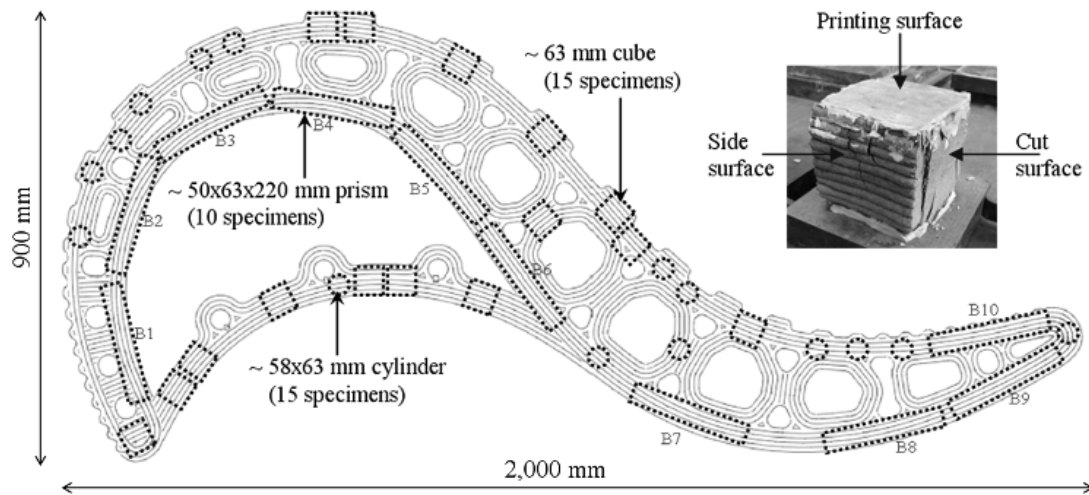


209

210 Figure 2. Cutting diagram and testing directions for nine 100 mm cube specimens
211 extracted from the 350x350x120 mm slab.

212

213



214

215 Figure 3. Diagram showing positions of extracting printed specimens from a
216 multi-cellular curved bench and typical cube specimen

217

218

219 Additionally, fifteen 58 mm diameter cores, fifteen 63 mm cut cubes and ten 50 x 220
220 mm width x length prisms were extracted from a 63 mm thick trial print of a curved
221 component to understand the performance of printed concrete under compressive
222 and flexural loading (Figure 3). All cylinder were tested perpendicular to the printing
223 surface while cube specimens were tested in three orientations: 3 perpendicular with
224 a cut surface (loading direction I), 9 perpendicular to the printing surface (loading
225 direction II) and 3 perpendicular with a side surface (loading direction III), as shown
226 top-right of Figure 3. The loading rate was also 0.4 N/mm². The full-scale print of the
227 bench has been shown in elsewhere [7, 8].

228

229

230 2.3.3. Flexural strength

231

232

233 Flexural strength was also measured in both mould-cast and printed states.

234 100x100x500 mm slabs were mould-cast, removed after one day and then cured in a

235 20°C water tank up to 28 days. For printed specimens, three 500x350x120 mm slabs

236 were printed and cured under damp hessian. Three 100x100x400 mm beams and

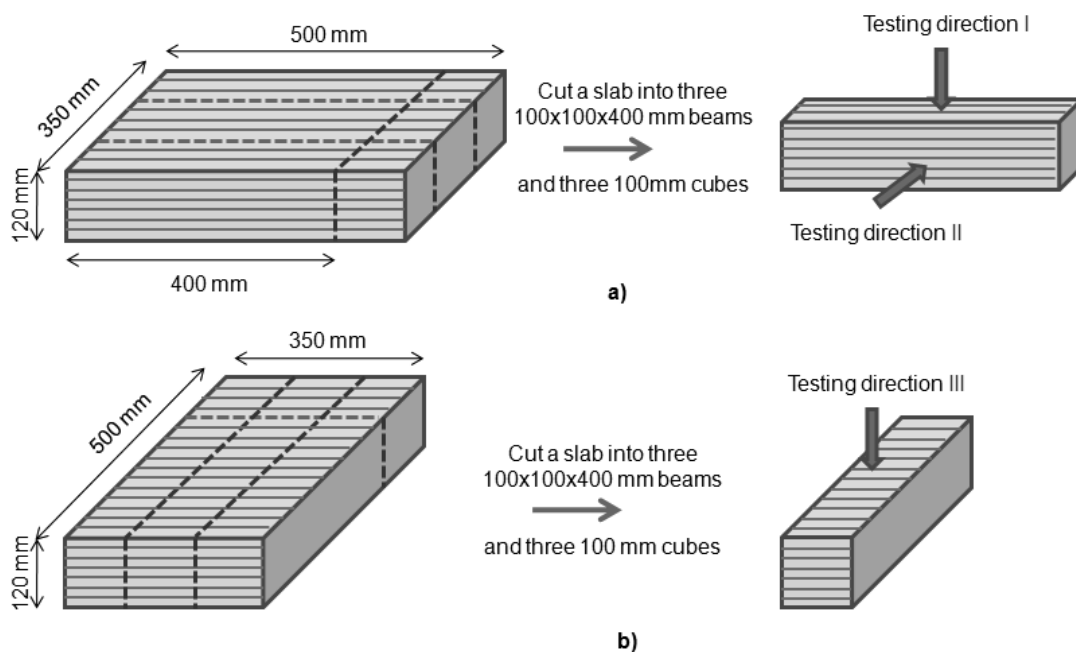
237 three 100 mm cubes were extracted from each slab at 28 day age. Slabs 1 and 2

238 were printed and cut as depicted in Figure 4a while slab 3 was printed and cut as

239 depicted in Figure 4b. Cube and beam specimens extracted from slabs 1, 2 and 3

240 were tested in directions I, II and III, respectively.

241



242

243 Figure 4. Diagram of cutting slabs and testing flexural strength

244

245

246 All beam specimens were tested under 4-point bending with a span of 300 mm,

247 complying with BS EN 12390-5:2009 [15].. An additional ten 50x63x220 mm beam

248 specimens extracted from the trial printed component (Figure 3) were also tested to
249 further understand anisotropy of the flexural performance of printed concrete.

250

251

252 *2.3.4. Tensile bond strength*

253

254

255 A critical characteristic of this printing process is the bond between layers, which can
256 influence the structural performance, particularly when the process temporarily stops
257 between layers. The influence of time between printing layers was investigated (in
258 increments of 15, 30 minutes, 1, 2, 4, 8, 18 hours and 1, 3, 7 days) by a direct
259 tension test on cylindrical cored specimens. The direct tensile strength was also
260 measured as a control using the same size of specimens and testing procedures.

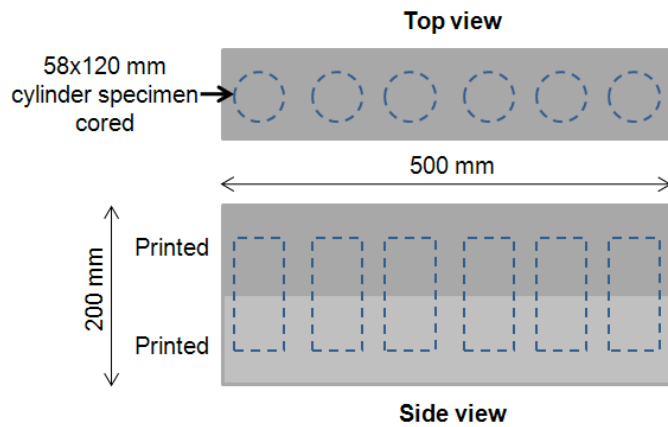
261

262

263 To prepare the cored cylinder specimens, a 100x100x500 mm beam was printed.
264 Then, after a time gap, another 100x100x500 mm beam was printed on top. The
265 components were then covered with damp hessian and plastic sheeting for a day
266 before being moved to a laboratory storage area where the same curing regime was
267 maintained up to 28 days. Six 58 mm diameter x 120 mm height cylinder specimens
268 were cored at the middle of each bonded beam component (Figure 5).

269

270



a) Coring six 58x120 mm cylinder specimens from a beam bond component b) Testing tensile bond strength

271 Figure 5. Arrangement for testing tensile bond strength

272

273

274 The cored cylinder specimens were tested in accordance with BS EN 14488-

275 4:2005+A1:2008 [16]. Two 58x25mm diameter x thickness steel dollies were glued to

276 the ends of each cylinder specimen with a rapid curing, high strength adhesive.

277

278 2.3.5. Void measurement

279

280

281 One of the characteristics of this concrete printing process is the voids that can form

282 between filaments (Figure 1), which might affect the hardened properties

283 significantly. The voids in the range of 0.2 – 4.0 mm size were quantified using

284 “Image Tool” processing and analysis software to better understand the effects on

285 the hardened performance of the printing concrete.

286

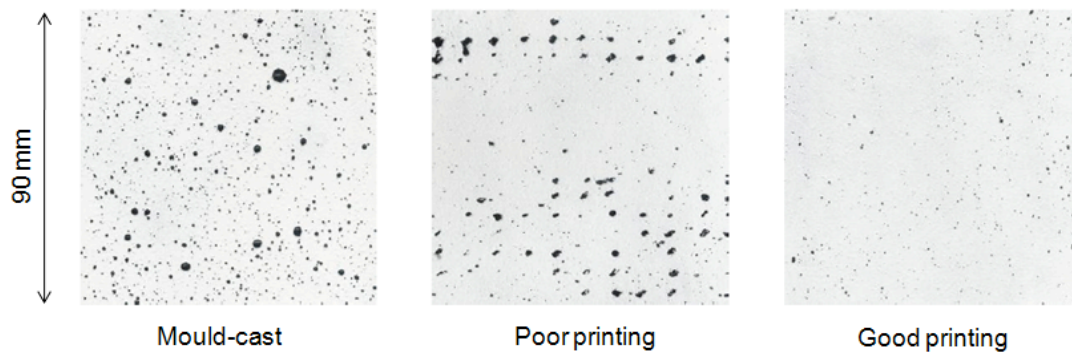
287

288 Void measurement was carried out in three specimen groups of mould-cast , poor

289 printing and good printing (Figure 6), each specimen having a 90x90 mm² surface.

290

291



292

293 Figure 6. Three typical specimens for void measurement

294

295

296 Surfaces were cleaned and sprayed with a black paint. Once dry, a white paint was
297 rolled on to reveal the voids that retained the black colour. The surface was
298 subsequently scanned and the image transferred to a void measuring software
299 “Image Tool” which counted the number of voids and their area.

300

301

302 2.3.6. Drying shrinkage

303

304

305 As the printing process fabricates without formwork, the surface area in contact with
306 air is large and this could accelerate drying shrinkage due to water evaporation, and
307 consequently increase the risk of cracking. Mould cast 75x75x229 mm beams
308 complying with BS EN 12617-4:2002 [17] were monitored over six months in three
309 curing conditions: water immersed, covered in damp hessian with a plastic sheet
310 wrapped and in a climatic chamber (20°C and 60% relative humidity). Each group
311 comprised five specimens.

312

313

314 **3. Results and Discussion**

315

316

317 **3.1. Density**

318

319

320 The average density (mould-cast) of the optimum mix was 2,250 kg/m³ Whilst that of
321 well-printed specimens was a little higher at 2,350 kg/m³ This was probably because
322 the concrete hopper was gently vibrated before delivery of the fresh concrete, and
323 the pipe and pump system also provided a small pressure during extrusion. A similar
324 trend occurred in a previous study on wet-spayed mortars [23, 24]. Although this high
325 performance printing concrete has only a sand aggregate, the density is much higher
326 than that of ordinary mortars (1,800 kg/m³) and sprayed mortars [23] (i.e. 1,800 –
327 2,000 kg/m³ on average). The high density is also attributed to the grading and
328 homogeneity resulting in high strengths and low shrinkage.

329

330

331 **3.2. Compressive strength**

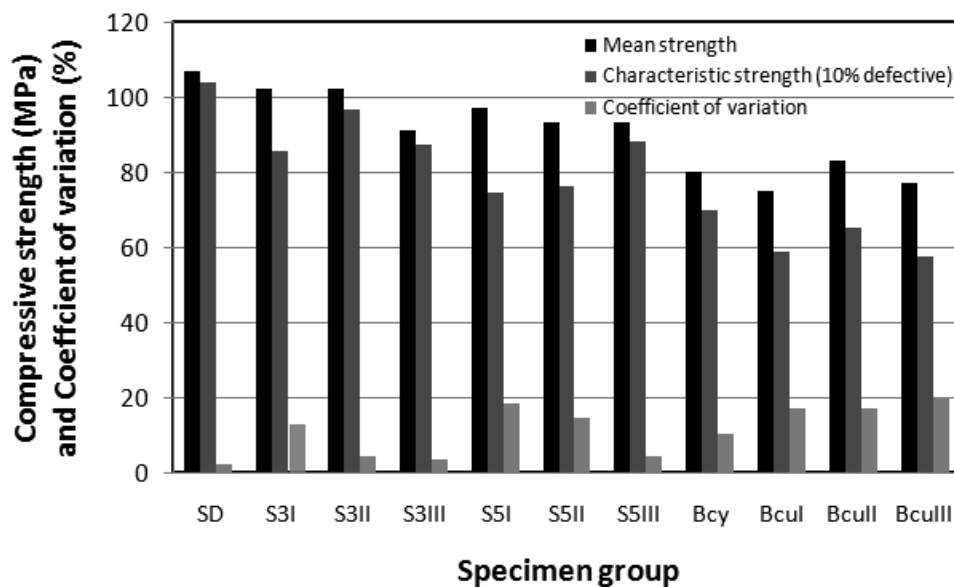
332

333

334 The mould-cast cube compressive strength at 28 days was typically 107 MPa but
335 varied with the admixtures and their dosages. The superplasticiser appeared to delay
336 the hardening of concrete at an early age. However, as expected and also in
337 agreement with previous work [21, 22], at 7 days and 28 days the specimens with 1-2
338 % superplasticiser had higher strength compared with 0.5 % superplasticiser.
339 Without superplasticiser the fresh concrete became stiff and then could not be
340 printed so the compressive strength was not determined. Over 1% retarder reduced

341 significantly the compressive strength at early ages, i.e. 1 and 7 days. Indeed 1.5-2%
 342 retarder resulted in no measurable compressive strength at 1 day. By 28 days, the
 343 retarder effect appeared to have disappeared, the compressive strengths of all mixes
 344 being approximately 100 MPa. The accelerator increased the compressive strength
 345 at one day significantly: by 70% with 3-5% and 40% with 1% accelerator. However,
 346 by 7 days, this enhancement had disappeared and by 28 days the strengths of 3-5%
 347 accelerator specimens were lower than that of 1% accelerator specimens.
 348 Testing of printed samples in various directions relative to the layers revealed a
 349 strength from 75 to 102 MPa (see Figure 11 which includes a comparison with mould
 350 cast equivalents).

351
 352
 353



354
 355
 356
 357

358 *Key:*

359 SD – standard 100 mm mould-cast cubes

Figure 11. Equivalent 100mm cube compressive strengths of printed concretes compared with mould-cast specimens

360 S3I, S3II, S3III – 100 mm cubes extracted from the 350x350x120 mm slab, tested in
361 loading direction I, II and III (see Figure 2)
362 S5I, S5II, S5III – 100 mm cubes extracted from three 500x350x120 mm slabs, tested
363 in loading direction I, II and III (see Figure 4)
364 Bcy – 58x63 mm cylinders cored from the trial curvy bench, (see Figure 3)
365 Bcul, Bcull, Bculll – 63 mm cubes extracted from the trial curvy bench, tested in
366 loading direction I, II and III (see Figure 3)

367

368

369 The average compressive strengths of the 100 mm cube specimens extracted from a
370 350x350x120 mm slab were 102 MPa in direction I (specimens 1, 2, 3) and the same
371 in direction II (specimens 4, 5, 6). In direction III it was 91 MPa (specimens 7, 8, 9).
372 Compared with the standard mould-cast compressive strength, the printed concrete
373 strength was similar in directions I and II and 15% lower in direction III. The nine 100
374 mm cube specimens tested in the series of three 500x350x120 mm slabs, depicted in
375 Figure 4, had an average compressive strengths of 97 MPa in direction I and 93 MPa
376 in directions II and III. The printed strength was thus 9% lower in direction I and 13%
377 lower in directions II and III, respectively. The results confirmed that a correctly
378 executed extrusion process introduces relatively little anisotropy in terms of
379 compressive strength, although it appears that loading in the plane of the layers
380 (directions II and III) can reveal a small reduction, presumably associated with shear
381 induced by platen friction exploiting any flaws at the bead boundaries.

382

383

384 However, the compressive strength reduced in the samples extracted from the print
385 of the curvy shape (the series of fifteen 58x120 mm cylinders and fifteen 63 mm
386 cube specimens). The equivalent cube compressive (converted using BS EN
387 12504:1-2009 [27] and an empirical relation [28]) varied from 75 to 83 MPa, i.e. up

388 30% less than the control. Additionally, the coefficients of variation of printed
389 specimens of 17-20% were significantly higher than that of standard cubes (2%).
390 Observation from the testing of this series revealed voids between the curved
391 filaments that are likely to have been the cause of the lower compressive capacity.

392

393

394 **3.3. Flexural strength**

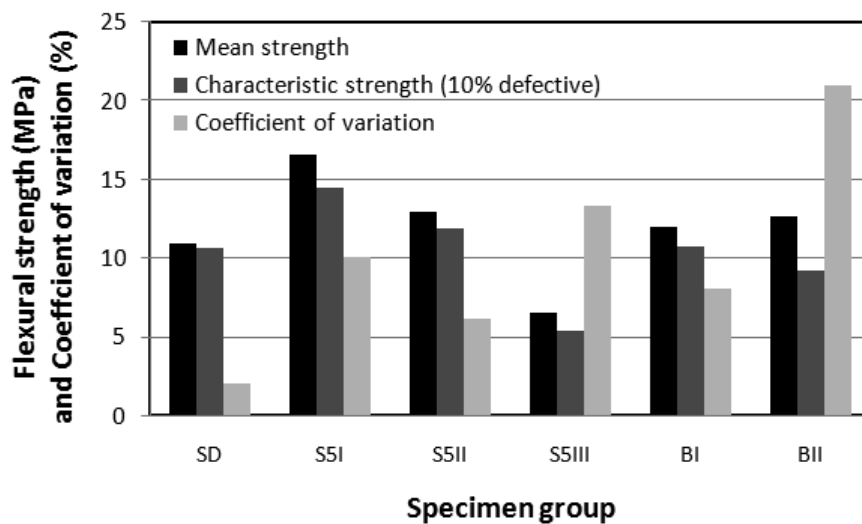
395

396

397 The average flexural strength of the mould-cast beams was 11 MPa (Figure 12), i.e.
398 approximately 10%, of compressive strength, agreeing with other research on high
399 strength concretes [29-31].

400

401



402

403 Figure 12. Flexural strengths of printed concrete compared with standard mould-cast
404 concrete

405

406 *Key:*

407 SD – standard 500x100x100 mm mould-cast beams

408 S5I, S5II, S5III – 400x100x100 mm beams extracted from three 500x350x120 mm
409 slabs, tested in loading direction I, II and III (Figure 4)

410 BI, BII – 220x63x50 mm beams extracted from the trial curvy bench, tested in loading
411 direction I and II (Figure 3)

412

413

414 The flexural strength of printed concrete varied with testing orientation. In the series
415 extracted from three slabs 500x350x120 mm, the strengths in loading directions I and
416 II (16 and 13 MPa respectively), were higher than that of the standard mould cast
417 material (11 MPa). The flexural strength is determined by the central bottom area of
418 beam specimens where the maximum tensile stress occurs. The concrete that
419 carried load in the testing direction I was at the bottom of the slab printed and this
420 area was probably well-compacted. The water-binder ratio of the lower concrete
421 layers would also have been reduced if water bled out of the base layer. The
422 combined effect would increase the loading capacity of the lower layers resulting in a
423 higher flexural strength. The beams tested in direction III had a much lower average
424 strength (7 MPa). This is because of the anisotropy resulting from the printing
425 process where, in this case, the load was applied in the plane of the boundaries
426 between filaments and the strength is thus highly dependent on the inter-layer bond
427 strength.

428

429

430 The flexural strength of smaller printed beams extracted from the curvy component (
431 was slightly higher than the control. The mean strength of 5 beams loaded in
432 direction I was 12 MPa and of 5 beams in direction II was 13 MPa. However these
433 values are lower than in the same directions of the printed slabs reflecting the
434 variation in printing quality and following the same trend as for compressive strength.

435 This is reinforced by the coefficients of variation of the printed specimens of up to
436 21% which were much larger than that of the mould-cast standard (2%).

437

438

439 **3.4. Tensile bond strength**

440

441

442 The tensile bond strength was investigated with 11 groups of specimens with a
443 varying time gap between the older and newer part. The results are compared with
444 the direct tensile strength of similar specimens and testing procedure in Figure 13.

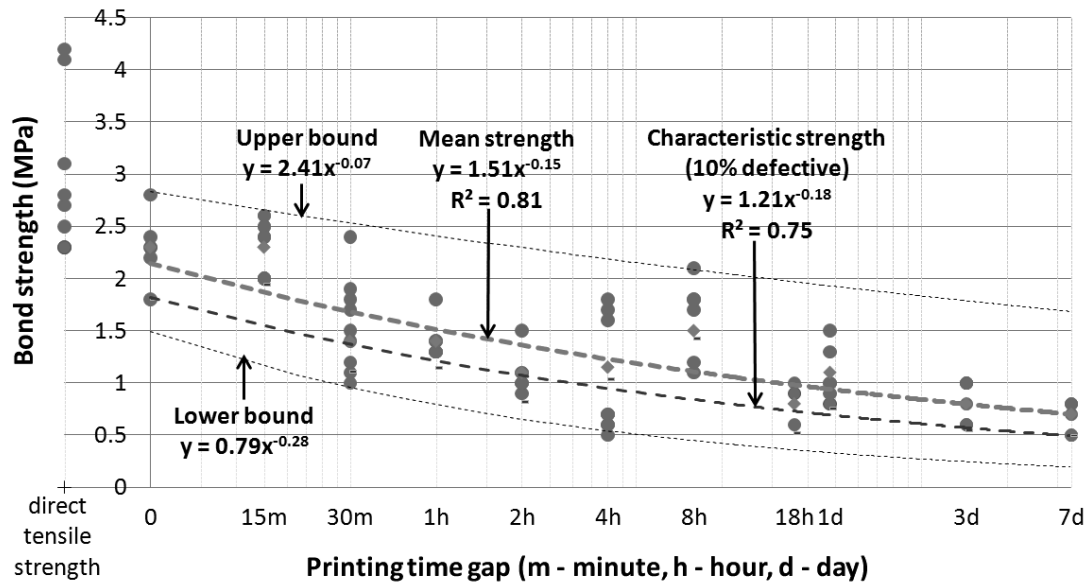
445

446

447 The results were quite variable, with coefficients of variation of 5 to 30%. This was
448 expected given the nature of the layered extrusion process and the well established
449 more general discussions concerning measurement of direct tensile strength [29] and
450 tensile bond testing of concrete repairs [32]. It is thought that such specimens are
451 more seriously affected by non-uniform shrinkage in comparison with other types of
452 test specimens.

453

454



455

456 Figure 13. Variation of tensile bond strength with printing gap and comparison with
 457 direct tensile strength

458

459

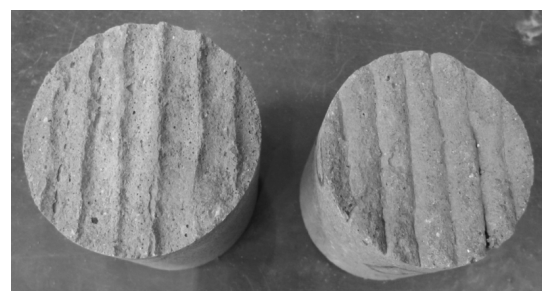
460 The failure stress was lower than the average tensile strength of 3.0 MPa, reducing
 461 on average from 2.3 MPa with printing time gaps of 0 and 15 minutes to 0.7 MPa for
 462 the 7 day gap. The specimens with a 0 and 15 minute time gap failed in the material
 463 (Figure 14a) and thus the bond strength could not be determined but is higher than
 464 the measured values.

465

466



a) 15 minute gap specimen



b) 4 hour gap specimen

467 Figure 14. Failure mode (broken surfaces) of tensile bond specimens

468

469

470 All specimens with a gap over 15 minutes failed at the interface between older and
471 newer parts (Figure 14b). Between a 30 minute and 7 day time gap the average bond
472 strength was 53% and 77% lower than the control. This reduction with increasing gap
473 in printing time was expected as the adhesion reduced. However, most of the results
474 comfortably exceeded the Concrete Society recommended minimum bond strength
475 of 0.8 MPa [23], and are well above the 0.4 to 0.9 MPa in a case study of a high
476 performance concrete bridge deck overlay [33]. They are similar to published bond
477 strengths of repair mortars and concretes of 0.8 to 2.3 MPa [23, 32, 34]. The trend
478 lines suggest that characteristic bond strengths of 0.8, 1.0 and 1.2 MPa will be
479 achieved with time gaps of 8, 3 and 1 hours respectively. A more demanding 1.5
480 MPa would restrict the printing time per layer to around 15 minutes.

481

482

483 **3.5. Void structure**

484

485

486 The anisotropy affecting the hardened properties including the compressive, flexural
487 and tensile bond behaviour was supported by the results of the void measurement.
488 These revealed 3.8% voids (0.2 – 4.0 mm size) in mould-cast specimens whilst 4.8%
489 formed in the poorly printed concrete and only 1.0% voids in the well printed
490 concrete. Respectively, the density results were 2,250, 2,260 and 2,350 kg/m³ for
491 mould-cast, poor printing and good printing. Although the void content of the poorly
492 printed concrete (4.8%) was greater than that of the mould-cast (3.8%) the density
493 was higher, implying a higher density. The content of voids less than 0.2 mm
494 diameter in the printed concrete is likely to be smaller than that of mould-cast
495 concrete.

496

497

498 The distribution of voids in the three concrete groups, Figure 15, clearly shows that
499 the area of small voids (0.2 – 1.6 mm) in mould-cast concrete was very much greater
500 than that of both poor and good printing concrete. The poorly printed had more large
501 voids (1.6 - 4.0 mm) compared with mould-cast concrete and are mostly located
502 between printed filaments (Figure 6). Once these were eliminated by correctly
503 controlling the printing path and concrete rheology, the density increased as seen in
504 the well printed concrete (2,350 kg/m³) that is representative of the specimens
505 prepared for the other hardened property tests. The distribution of voids in good
506 printing concrete agreed well with this as the area of 0.2 – 4.0 mm voids was
507 significantly lower than both mould-cast and poor printing concrete.

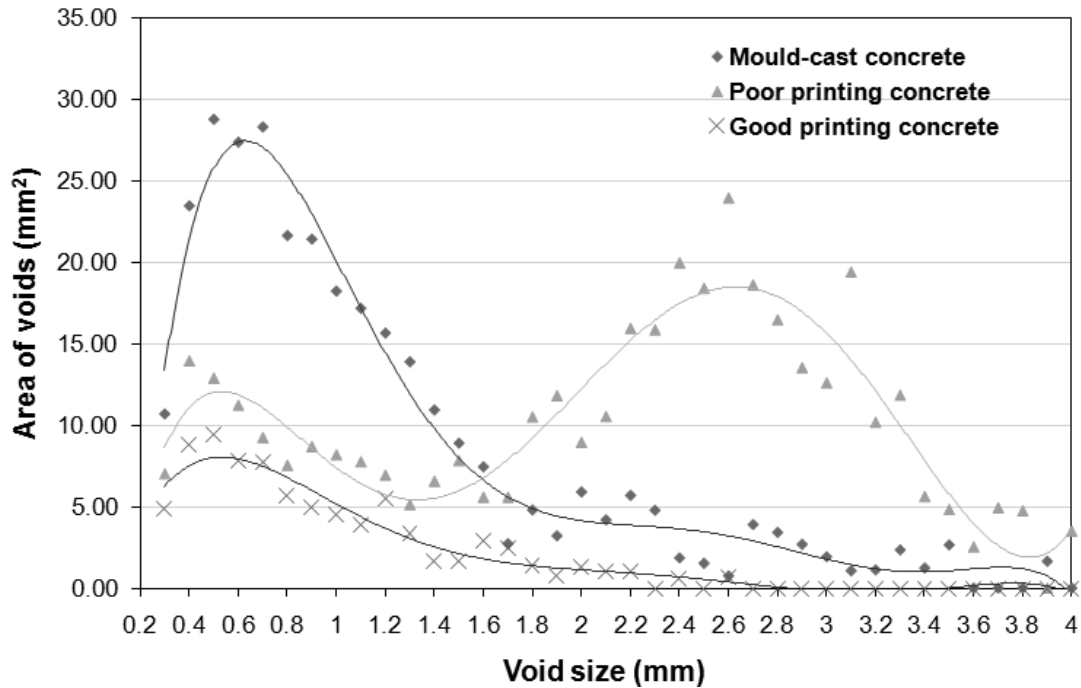
508

509

510 Whilst the tests reported here are not extensive they provide important insights into
511 the nature of this extrusion process and the influence on the structure of the resulting
512 matrix and hence mechanical performance.

513

514



515

516 Figure 15. Distribution of voids in three concrete groups

517

518

519 3.6. Drying shrinkage

520

521

522 As expected, the concrete cured in water shrank the least. It expanded up to 67

523 microstrain in first two days and then shrank to 177 microstrain by 28 days.

524 Thereafter the shrinkage rate noticeably reduced with only 62 microstrain between 30

525 and 180 days. (Figure 16. The influence of damp hessian was monitored in two

526 phases. During the first 60 days it was watered and wrapped in plastic sheeting so

527 the relative humidity was around 100% but the temperature varied in a range of 15 to

528 25°C depended on the ambient conditions. The shrinkage of 252 microstrain by 70

529 days was relatively low. In the second phase when the hessian was not watered and

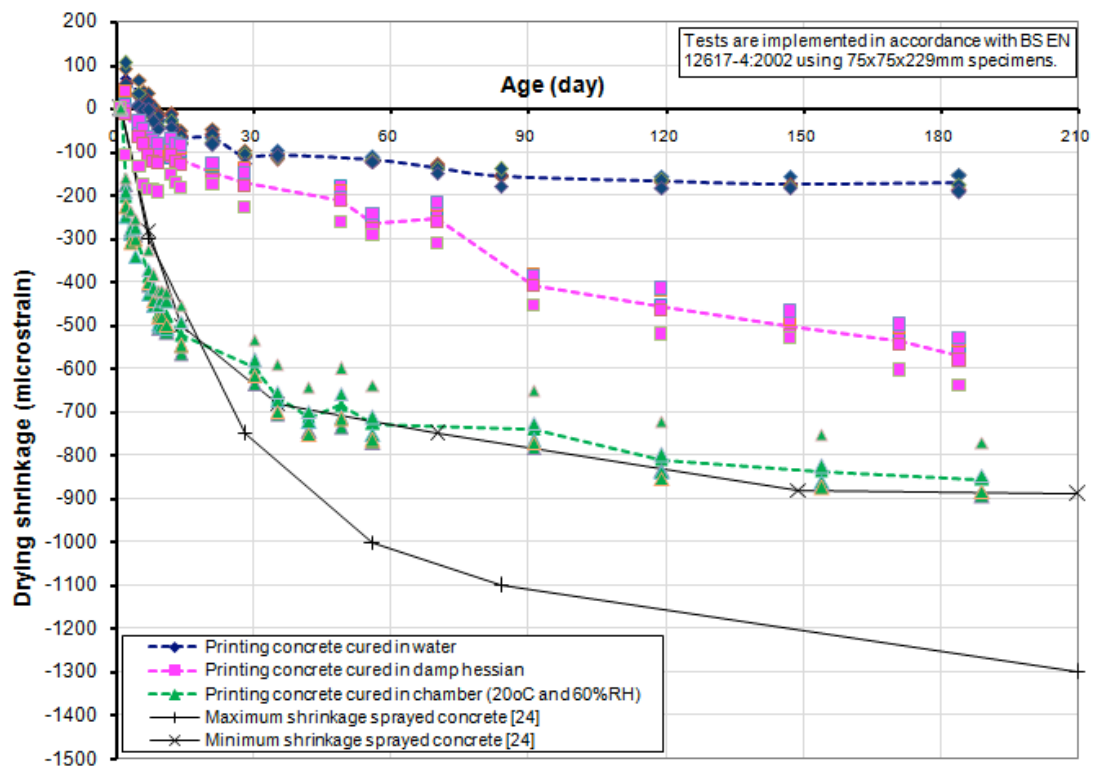
530 the plastic sheeting removed, the shrinkage rate increased from 70 to 90 days (408

531 microstrain), then gradually slowed to 570 microstrain at 184 days. The concrete in

532 the climatic chamber at a consistent 20°C and 60% relative humidity shrank quickly in
533 first 30 days by 597 microstrain then gradually slowed to 855 microstrain at 189 days.

534

535



536

537 Figure 16. Drying shrinkage in three curing conditions with comparison to sprayed
538 concretes

539

540

541 The higher shrinkage, by a factor of 3-4 times larger than that cured at 100% relative
542 humidity, agrees reasonably well with the research by Bissonnette et al. [35] who
543 observed the influence of relative humidity on the drying shrinkage of a mortar and
544 obtained the results of approximately 300, 800 and 1400 microns for the specimens
545 cured in 92, 75 and 48% relative humidity, respectively. Brooks et al. [36] also found
546 greater shrinkage in 30 MPa compressive strength mortar specimens cured under
547 plastic sheeting (approximately 2,200 microns) compared with water (approximately

548 1,000 microns). The results are thus as would be expected of cementitious system
549 sensitive to changes in relative humidity, which disturb the equilibrium between
550 adsorbed water and vapour pressure [37].

551

552

553 The shrinkage in all three conditions was notably lower than that of sprayed mortars
554 [23, 24] considered to be low shrinkage materials, when cured at 20°C and 50%
555 relative humidity. The optimum particle grading, low water/binder ratio and fly ash
556 addition thus appeared to be helpful in lowering the shrinkage of the high
557 performance printing concrete. This is a notable advantage for a manufacturing
558 process without formwork where the complete surface of components is exposed.

559

560

561 **4. Conclusions**

562

563

564 A high-performance concrete has been successfully developed for a digitally-
565 controlled printing process which can build architectural and structural components
566 without formwork. The concrete in the mould-cast state had high strengths (107 and
567 11 MPa compressive and flexural strength respectively), low drying shrinkage and a
568 density of 2,250 kg/m³. The printing process increased the density up to 2,350 kg/m³,
569 although, as anticipated, the layering process can introduce small linear voids in the
570 interstices between the extruded filaments. The gentle vibration of concrete container
571 and the small pump pressure in the extrusion process probably reduced the volume
572 of voids, resulting in the increase in density. Furthermore, poor printing could result in
573 a lower density (2,260 kg/m³) with 1.6 – 4.0 mm voids. located principally at the
574 intersection of filaments

575

576

577 The hardened properties were inevitably affected by any anisotropy in the layered
578 structure of freeform components. Up to 30% reduction in compressive strength was
579 observed in a curvy-shape full-scale bench structure. The potential improvement is
580 implied by the higher strengths of around 91-102 MPa found in the specimens
581 extracted from straight-line printed slabs. Here the reduction was only 5-15%,
582 depending on the orientation of the loading relative to the layers, the lowest strengths
583 occurring as would be expected when loading in planes parallel to the layers.

584

585

586 In terms of tensile properties, the flexural strength was significantly higher (13-16
587 MPa) than the mould-cast control (11 MPa) when tension was aligned with the
588 extruded filaments. However, as expected, the flexural strength was significantly
589 reduced when loaded to cause tension between (perpendicular) the layers (by up to
590 36%) but still high relative to conventional precast concretes at 7 MPa. A similar
591 trend was observed in the measurement of direct tensile strength, reducing from 3.0
592 MPa in the mould-cast control to 2.3 MPa, the difference between the indirect and
593 direct values following well-established behaviour.

594

595

596 The bond strength between the layers of printed concrete is perhaps the critical
597 mechanical property of material produced by an AM process, creating potential flaws
598 between extrusions that induce stress concentrations. This is highly dependent on
599 the adhesion which is a function of the time between extrusions. There is a careful
600 balance required, as with sprayed concretes, keeping the materials sufficiently open
601 for adhesion, but developing sufficient rigidity to support its self-weight. The
602 optimised mix contained appropriate proportions of superplasticizer and retarder.

603

604

605 The tensile bond strength inevitably reduced as the printing gap between layers
606 increased. Where this was kept to 15 minutes the bond was greater than the tensile
607 capacity of the material. A gap of 30 minutes or more resulted in bond failure at the
608 interface and a relationship between characteristic bond strength and time has been
609 established.

610

611

612 In macro terms, a variety of freeform building components were printed, including a
613 large-scale curvy bench with weight of approximately 1 tonne [7, 8]. Whilst drying
614 shrinkage of such parts is inevitably a concern, the data indicates acceptable levels
615 when good curing is provided. The research has thus demonstrated the potential of
616 concrete printing as a viable new production process that can introduce greater
617 geometric freedom into the design process as well as offering a novel means of
618 manufacture that could avoid the need to mass produce identical concrete parts with
619 limited numbers of variants. Further research is required to assess the structural
620 behaviour of such components under simulated service conditions as well as to
621 establish their durability, particularly in relation to any adverse effects of the layering
622 process.

623

624

625 **Acknowledgements**

626

627

628 This project was funded by the Engineering and Physical Sciences Research Council
629 under grant EP/E002323/1 through the IMCRC at Loughborough University. The
630 authors acknowledge the supply of materials from Hanson Cement, Weber (St
631 Gobain) and BASF and the assistance in designing the freeform components from

632 Foster & Partners and Buro Happold. We are also grateful for the laboratory
633 assistance of John Webster, Gregory Courtney, Harriet Mather, Jonathan Hales and
634 David Spendlove.

635

636

637 **References**

638

639

640 [1] R. A. Buswell, R. C. Soar, A. G. F. Gibb, T. Thorpe, Freeform construction: Mega-
641 scale rapid manufacturing for construction, *Automation in Construction*, 16 (2007)
642 224-231.

643 [2] S. Lim, T. Le, J. Webster, R. Buswell, S. Austin, A. G. F. Gibb, T. Thorpe,
644 Fabricating construction components using layer manufacturing technology,
645 Proceedings of International Conference on Global Innovation in Construction,
646 Loughborough, UK, 2009, pp. 512-520.

647 [3] H. Okamura, M. Ouchi, Self-compacting concrete, *Journal of Advanced Concrete*
648 *Technology*. 1 (2003) 5-15.

649 [4] RILEM Technical Committee, Final report of RILEM TC 188-CSC "Casting of self
650 compacting concrete", *Materials and Structures*, 39 (2006) 937-954

651 [5] S. A. Austin, P. Robins, C. I. Goodier, The rheological performance of wet-
652 process sprayed mortars, *Magazine of Concrete Research*, 51 (1999) 341-352.

653 [6] S. A. Austin, P. Robins, C. I. Goodier, Construction and Repair with Wet-Process
654 Sprayed Concrete and Mortar, Technical Report 56, The Concrete Society, UK,
655 2002, p. 44.

656 [7] T. T. Le T, S. A. Austin, S. Lim, R. Buswell, A. G. F. Gibb, T. Thorpe, Mix design
657 and fresh properties for high-performance printing concrete, *Materials and Structures*
658 (accepted in June 2011).

659 [8] T. T. Le T, S. A. Austin, S. Lim, R. Buswell, A. G. F. Gibb, T. Thorpe, High-
660 performance printing concrete for freeform building components, Proceedings of
661 International Fib Symposium on Concrete Engineering for Excellence and Efficiency,
662 Prague, Czech Republic, 2011, pp. 499-502.

663 [9] B. Khoshnevis, D. Hwang, K. Yao, Z. Yeh, Mega-scale fabrication by contour
664 crafting, International journal of Industrial and System Engineering 1 (2006) 301–320.

665 [10] Enrico Dini. “*D_Shape*.”, <http://www.d-shape.com>, accessed on 05th October
666 2011.

667 [11] A. M. Evans, R. I. Campbell, A comparative evaluation of industrial design
668 models produced using rapid prototyping and workshop-based fabrication
669 techniques, Rapid Prototyping Journal, 9 (2003) 344–351.

670 [12] J. Pegna, Exploratory investigation of solid freeform construction, Automation in
671 Construction, 5 (1997) 427–437.

672 [13] World Technology Evaluation Center, Inc., Additive / Subtractive manufacturing
673 research and development in Europe, WTEC Panel report, 2004, p. 154. [14] British
674 Standards Institution, BS EN 12390-3:2009 Testing hardened concrete -
675 Compressive strength of test specimens, Milton Keynes, UK, 2009, p. 15.

676 [15] British Standards Institution, BS EN 12390-5:2009 Testing hardened concrete -
677 Flexural strength of test specimens, Milton Keynes, UK, 2009, p. 11.

678 [16] British Standards Institution, BS EN 14488-4:2005+A1:2008 Testing sprayed
679 concrete - Bond strength of cores by direct tension, Milton Keynes, UK, 2008, p. 7.

680 [17] British Standards Institution, BS EN 12617-4:2002 Products and systems for the
681 protection and repair of concrete structures. Test methods. Determination of
682 shrinkage and expansion, Milton Keynes, UK, 2002, p. 14.

683 [18] British Standards Institution, BS EN 12390-7:2009 Testing hardened concrete -
684 Density of hardened concrete, Milton Keynes, UK, 2009, p. 10.

685 [19] S. Erdogdu, Effect of retempering with superplasticizer admixtures on slump loss
686 and compressive strength of concrete subjected to prolonged mixing, Cement and
687 Concrete Research, 35 (2005) 907-912.

688 [20] V. Morin, F. C. Tenoudjia, A. Feylessoufib, P. Richard, Superplasticizer effects
689 on setting and structuration mechanisms of ultrahigh-performance concrete, Cement
690 and Concrete Research, 31 (2001) 63-71.

691 [21] American Concrete Institute, ACI 212.4R-93 (Reapproved 1998) Guide for the
692 Use of High-Range Water-Reducing Admixtures (Superplasticizers) in Concrete,
693 1998, p. 10.

694 [22] UK Cement Admixtures Association, Admixture Technical Sheet – ATS 2
695 Superplasticising / High range water reducing, 2006, p. 5..

696 [23] S. A. Austin, P. Robins, C. I. Goodier, The performance of hardened wet-process
697 sprayed mortars, Magazine of Concrete Research, 52 (2000) 195-208.

698 [24] C. I. Goodier, S. A. Austin, P. Robins, Low-volume wet-process sprayed
699 concrete: hardened properties, Materials and Structures, 41 (2008) 99-111.

700 [25] UK Cement Admixtures Association, Admixture Sheet – AS 3 Set Retarding. Set
701 Retarding / Water Reducing / Plasticising. Set Retarding / High Range Water
702 Reducing / Superplasticising, 2006, p. 4.

703 [26] UK Cement Admixtures Association, Admixture Sheet – ATS 4 Accelerating
704 admixtures, 2006, p. 4..

705 [27] British Standards Institution, BS EN 12504-1:2009 Testing concrete in structures
706 Part 1: Cored specimens — Taking, examining and testing in compression, 2009, p.
707 8.

708 [28] J. R. Del Viso, J. R. Carmona J R, G. Ruiz, Shape and size effects on the
709 compressive strength of high-strength concrete, Cement and Concrete Research, 38
710 (2008) 386–395.

711 [29] A. M. Neville, Properties of concrete, Longman group limited, England, UK,
712 1995.

713 [30] T. T. Le, Ultra high performance fibre reinforced concrete paving flags, PhD
714 thesis, University of Liverpool, UK, 2008, p. 405.

715 [31] S. Bhanjaa, B. Sengupta, Influence of silica fume on the tensile strength of
716 concrete, *Cement and Concrete Research*, 35 (2005) 743-747.

717 [32] S. A. Austin, P. Robins, Y. Pan, Tensile bond testing of concrete repairs,
718 *Materials and Structures*, 28 (1995) 249-259.

719 [33] Department of Transportation, United States, Tensile bond strength of a high
720 performance concrete bridge deck overlay - Field test report, Federal Highway
721 Administration, Office of Pavement Technology, Washington, USA, 2000, p. 10.

722 [34] K. H. Hindo, In-plane bond testing and surface preparation of concrete, *Concrete*
723 *International*, 12 (4) (1990) 46-48.

724 [35] B. Bissonnette, P. Pierre, M. Pigeon, Influence of key parameters on drying
725 shrinkage of cementitious materials, *Cement and Concrete Research*, 29 (1999)
726 1655–1662.

727 [36] J. J. Brooks, B. H. Abu Bakar B H, Shrinkage and creep of masonry mortar,
728 *Materials and Structures*, 37 (2004) 177-183

729 [37] K. Kovler, S. Zhutovsky, Overview and future trends of shrinkage research,
730 *Materials and Structures*, 39 (2006) 827–847.